MODELING OF GEOMETRIC MISTUNING IN BLADED ROTORS

N. Wagner, R. Helfrich
(INTES GmbH, Germany)

Abstract

Blisks also known as bladed disks are designed to be cyclic structures. However, tolerances in the manufacturing and assembling processes and wear originate a loss of symmetry. This phenomenon is called mistuning effect. These imperfections inherently influence the dynamic behaviour of the rotor. It turns out that they can drastically influence the forced response levels. These imperfections could cause large increases in stress and vibration amplitudes. Hence the demand for computationally effective methods to predict and quantify such systems is of great interest to the manufacturers of turbine engines. Due to the spatial confinement of vibration energy, certain blades in a mistuned system can suffer a significant in forced-response vibration amplitudes compared to the ideal (tuned) system. The mistuning effect is often idealized by a modification of mass and stiffness distribution inside the blades. It is often overlooked, that imperfections in the shape of the blades are unavoidable. Possible causes of this relationship are in-use wear, temperature fluctuations and manufacturing tolerances. Another factor which comes into play in the CAE field is the fact that the kind of meshing might introduce geometric perturbations with respect to the ideal shape. Usually a single sector is meshed and rotated to yield the full rotor model. However, this is a time-consuming task, since the number of nodes and their positions on the upper and lower interface of the sector have to fulfil certain criteria. Therefore, in many industrial applications a tetrahedral meshing tool is directly applied to a triangular surface mesh of the full rotor. A splitting of multiple eigenfrequencies is observed in that case. In this study we focus on geometric mistuning. The geometric mistuning is introduced by using so-called shape basis vectors. Hence, arbitrary perturbations might be independently applied to each sector of the bladed rotor. However, a linking of design variables is possible in order to reduce the number of shape variations. A sampling procedure is used to create a multidimensional map in the design space. This map can be used to study the influence of geometric mistuning effects on characteristic parameters of a rotordynamic analysis, i.e. real, complex eigenfrequencies and response amplitudes etc. A centrifugal impeller taken from the literature is used here to illustrate the procedure. Characteristic results like nodal diameter plots, Campbell diagrams and forced response amplitudes are compared with the ideal (i.e. cyclic symmetric) impeller. All computations are carried

out in PERMAS. PERMAS specific commands are highlighted by a preceding dollar sign and capital letters in the subsequent sections.

1. Overview

Geometric mistuning refers to inevitable variations in blade geometries, which arise during the manufacturing process, assembly tolerances and non-uniform wear during service. Mistuning parameters are usually described by random variables. New measurement techniques such as coordinate measurement machines (CMM) are used to detect deviations from design intent. CMMs collect data through a geometry traversing probe that obtains spatial data points at regular intervals. A principal component analysis is applied to create a reduced basis set of the manufacturing deviations Brown [4]. Garzon [6] investigated the impact of geometric variability on axial compressor performance. Sinha developed a modified modal domain analysis for reduced-order models of bladed rotors subjected to geometric mistuning. Extremely large mistuning is considered by Bhartiya [2]. Besides geometric mistuning, other sources of mistuning are stiffness and mass variations [11]. Due to the loss of cyclic symmetry, sector analysis cannot be performed.

2. Geometric mistuning

Geometric mistuning may be investigated from a statistical point of view due to its random characteristics. However, in this study we focus on a deterministic sampling procedure, where the shape of each sector can be varied on a regular grid of design variables. A wizard supports the set-up of the mesh morphing procedure. The shape basis vectors are calculated by PERMAS [12] and provided for visualization in VisPER [13]. The results of a shape modification can be exported as displacements for post-processing with the original model or as a new model with identical topology and modified coordinates. The design nodes can be interactively selected for each sector. It becomes evident that the number of necessary loops for the sampling procedure is given by

$$L = \prod_i n_{v,i} \,, \tag{1}$$

where $n_{v,i}$ denotes the number of discrete values specified for the i-th design variable. Therefore the number of design variables is limited to a small number for industrial models, i.e. blisks with many blades.

3. Equations of motion

The governing equations of motion that describes a rotor system in a co-rotating reference frame is given by

$$M\ddot{u} + (D + D_c)\dot{u} + \left(K + K_g + K_c\right)u = R(t), \qquad (2)$$

where M denotes the mass matrix, D the viscous damping matrix, D_c Coriolis matrix, K_c centrifugal stiffness matrix, K_g geometric stiffness matrix, K structural stiffness matrix and $R(t)$ external forces. The next step is the calculation of real eigenmodes $X = [x_1, \dots, x_r]$, including geometric and centrifugal stiffness matrices

$$MX = (K + K_g + K_c)X\,\Lambda, \qquad X \in \mathbb{R}^{n\times r} \qquad (3)$$

where r denotes the number of requested eigenfrequencies. The equations of motion are transformed into modal space by means of $u = X\,q$. The real and complex eigenvalue problems are repeatedly solved for varying shape parameters and varying speeds of the impeller

$$\lambda \begin{bmatrix} -\widetilde{M} & O \\ O & I_r \end{bmatrix} z = \begin{bmatrix} \widetilde{D} + \widetilde{D}_c & \widetilde{K} + \widetilde{K}_c + \widetilde{K}_g \\ I_r & O \end{bmatrix} z, \quad z = \begin{bmatrix} \lambda q \\ q \end{bmatrix}, \qquad (4)$$

since the system matrices vary with the shape parameters $p \in \mathbb{R}^s$. This task is realized by the SAMPLING procedure in one computational run.

Example

The example is taken from Wang et. al. [11]. The industrial impeller Fig. 1 consists of a cover component, a disk component and eleven blades. The material of the impeller is an alloy steel. Each sector consists of 5064 second-order tetrahedral elements. Therefore we ensure that the shape and the size of each of the blades are cyclically identical. The impeller was assumed to be restrained at the inner bore diameter. All geometrical and physical parameters are given in Table 1.

Table 1: Geometrical and physical parameters of the impeller

Inner diameter d_i [m]	0.096
Outer diameter d_o [m]	0.4
Young's modulus E [Gpa]	214.6
Density ρ [kg/m^3]	7850.
Poisson's ratio ν	0.3006

The first eleven eigenfrequencies of the initially cyclic symmetric impeller are given in Table 2. It turns out that mode 9 is missing in the reference paper by Wang et. al. [11]. The nodal diameter plot is given in Fig. 2. The modal assurance criteria (MAC) matrix measures the degree of proportion between two modal vectors in the form of a correlation coefficient. MAC is defined by

$$MAC(\Phi_r, \Phi_s) = \frac{|\, \phi_r^{\mathrm{T}}\, \Phi_s \,|^2}{(\phi_r^T\ \phi_r)(\phi_s^T\ \phi_s)} \quad , \tag{5}$$

where ϕ_r, ϕ_s are real eigenvectors. For $r = s$ the MAC value should be close to unity; for $r \neq s$ the MAC value should be low. However, in case of cyclic symmetric structures, modes with an identical number of nodal diameters are geometrically similar. Hence the MAC matrix can be used to identify modes with an identical number of nodal diameters. For this purpose logarithmically scaled MAC values are used in the graphical representation Fig. 3.

Table 2: First ten natural eigenfrequencies of the tuned impeller

Mode index	Nodal diameter	PERMAS f_i [Hz]	Wang et.al.
1	0	1046.64	1046.60
2	1	2112.98	2113.00
3	1	2112.98	2113.00
4	0	2568.72	2568.70
5	2	2706.62	2706.60
6	2	2706.62	2706.60
7	1	3429.87	3429.80
8	1	3429.87	3429.80
9	0	3646.76	----------
10	3	3816.40	3816.20
11	3	3816.40	3816.20

Mistuning has been introduced by varying the shape of the blades. For this purpose the surface normal displacement is modified by introducing so-called shape basis vectors at each blade. One or several inner nodes of the design element are selected as design nodes. Each movement of a design node leads to a smooth mesh modification in the whole design element. A mesh modification which is originated by a unit change of a single design variable is called shape basis vector. Thus geometric mistuning modifies both the mass and the stiffness matrices

of each sector by varying amounts. An element test is integrated in PERMAS, to restrict the mesh distortion to an allowable limit.

In order to reduce the number of 11 design parameters $p \in \mathbb{R}^{11}$ to only two, we assume that there are only two distinct nominal blades, type A and type B, arranged in the alternating pattern $ABAB \ldots A$ represented by p_1, p_2 as depicted in Fig. 4. The linking between different design variables is achieved by $DSVLINK. A wizard for shape optimization is available in VisPER and can be used to complete the finite element model with respect to the mesh morphing task. It provides guidance through the different steps of optimization modelling in a user-friendly way. The results of the mesh morphing process can be exported as displacements for post-processing with the original model or as new model with identical topology and modified coordinates.

The design parameters p_1, p_2 are uniformly distributed over a square grid $[-4,4] \times [-4,4]$. Overall 81 parameter combinations are available.

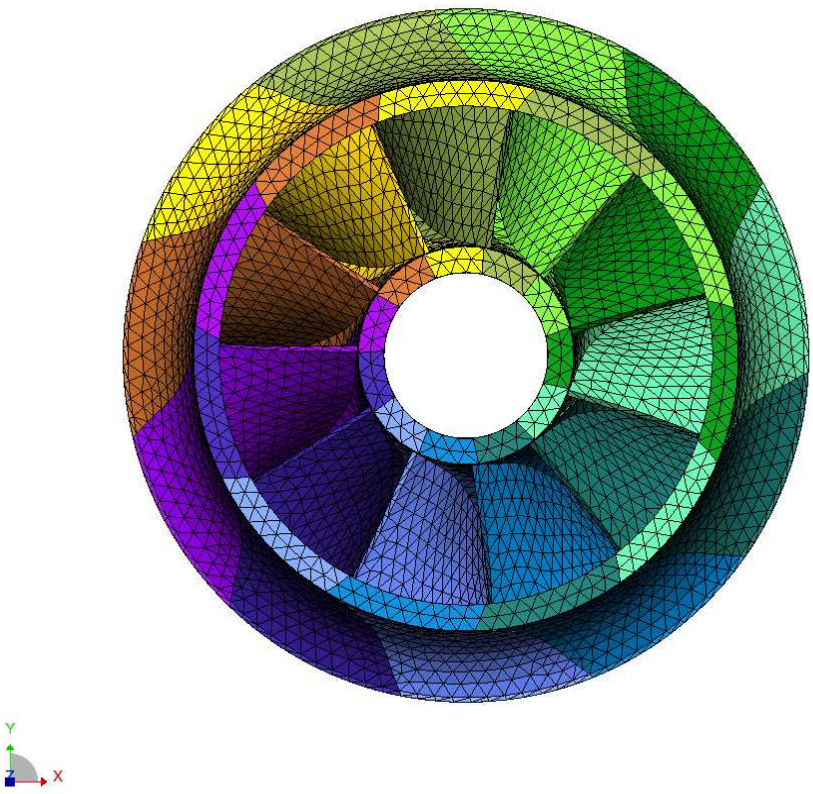

Figure 1: Industrial impeller. Each colour represents one sector.

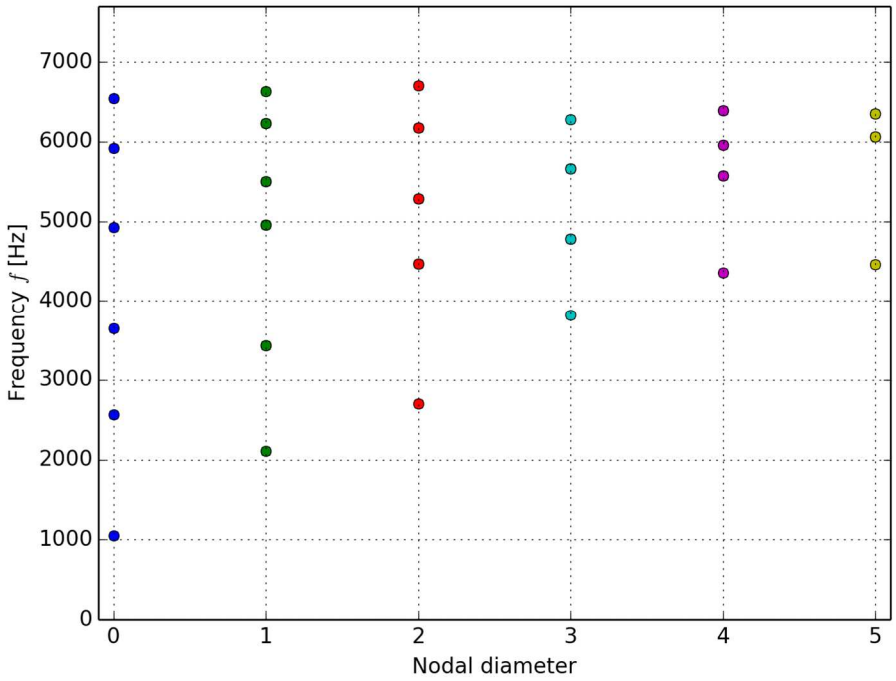

Figure 2: Nodal diameter plot of the nominal impeller

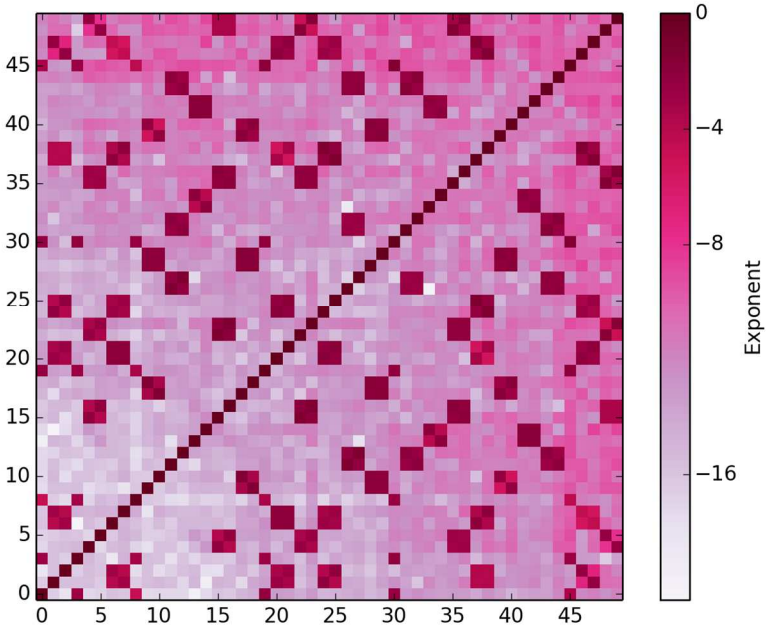

Figure 3: Modal assurance criterion logarithmic scale. Dark squares denote a strong correlation between eigenvectors.

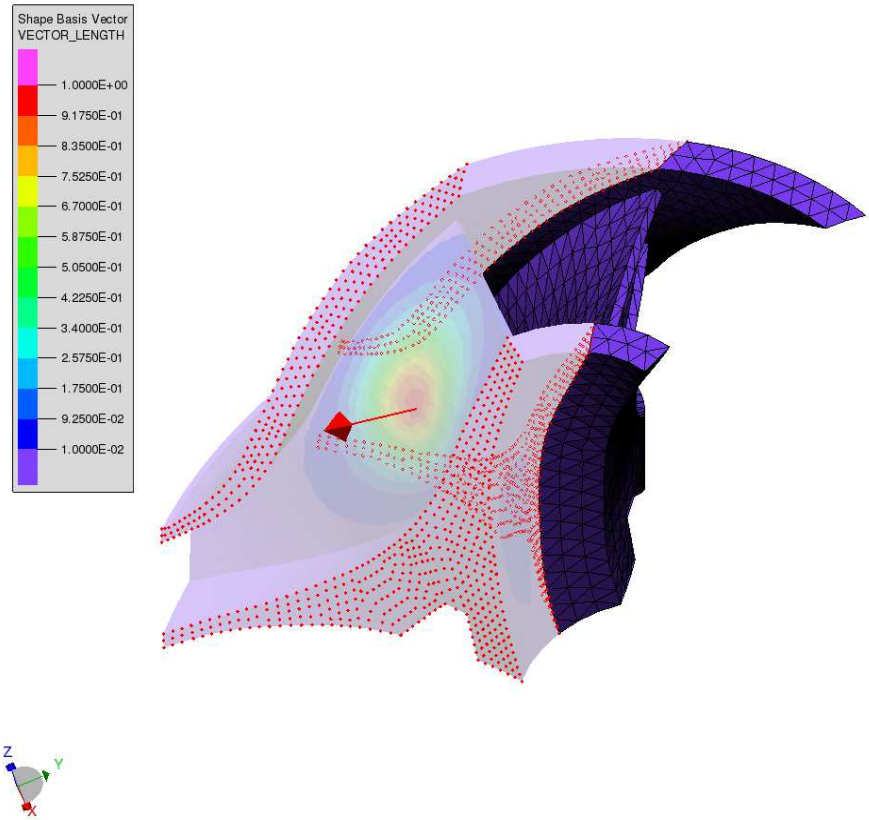

Figure 4: Design element and corresponding shape basis vector denoted by a red arrow. Red dots denote boundary/interface nodes of the design element/sector.

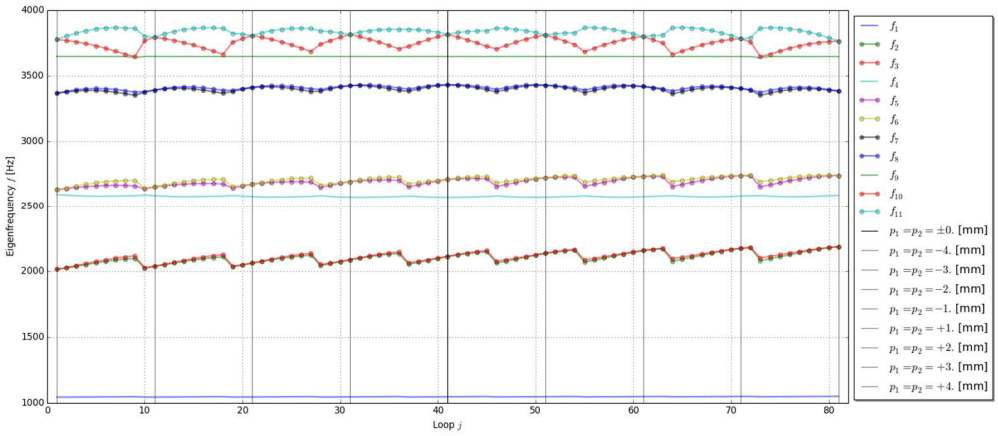

Figure 5: The first eleven eigenfrequencies of the impeller as a function of design variables. The vertical line at x=41 denotes the tuned (unperturbed) impeller.

The cyclic symmetry is also preserved at $x_i = 10\ (\ i - 1) + 1, i = 1, \ldots, 9$, where double eigenfrequencies are present. These parameter combinations are characterized by identical shape variations $p_1 = p_2 = p$. The design node itself is rotated for each sector in this study. That means, that the mesh modification is cyclic symmetric.

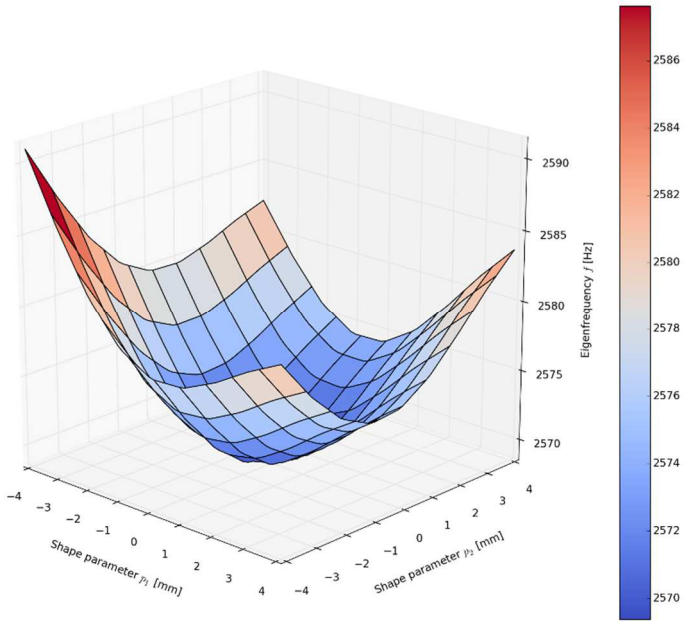

Figure 6: Fourth eigenfrequency as a function of shape parameters

A global minimum for the fourth eigenfrequency (Fig. 6) is achieved in the vicinity of the nominal settings, whereas the eighth eigenfrequency is maximized (see Fig. 7).

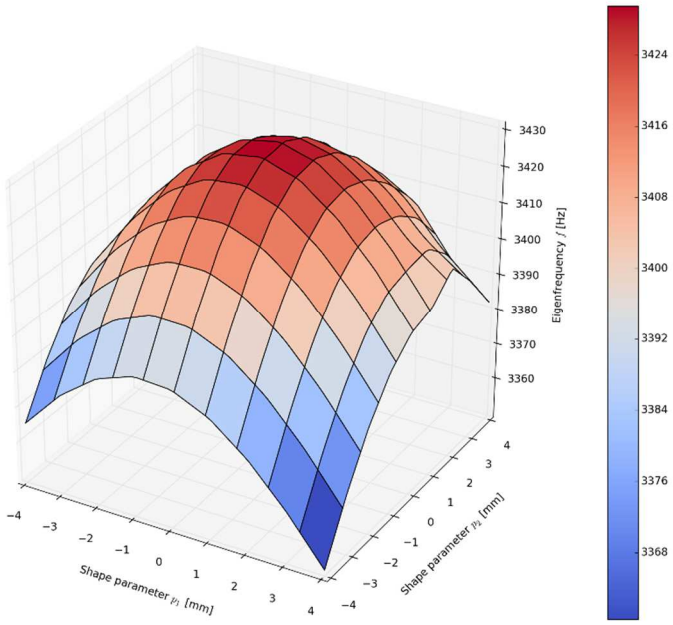

Figure 7: Eighth eigenfrequency as a function of shape parameters

4. Conclusions

The effects of geometric mistuning on the free response of initially cyclic symmetric structures is of great interest. All the necessary tools are provided by PERMAS/VisPER to perform a SAMPLING analysis in a seamless process chain. Sensitivities of system parameters such as eigenfrequencies with respect to geometric perturbations can be used for intentional mistuning.

5. References

[1] Beck, Joseph; Brown, Jeffrey; Cross, Charles, Slater, Joseph (2014), Component-mode reduced-order models for geometric mistuning of integrally bladed rotors. AIAA Journal, Vol. 52, pp. 1345--1356

[2] Bhartiya, Yasharth; Sinha, Alok (2013), Reduced order modelling of a bladed rotor with geometric mistuning: Alternative bases and extremely large mistuning. International Journal of Gas Turbine, Propulsion and Power Systems, Vol. 5

[3] Bhartiya, Yasharth; Sinha, Alok (2014). Accuracies of reduced order models of a bladed rotor with geometric mistuning, Journal of Turbomachinery. Vol. 136

[4] Brown, Jeffrey M.; Grandhi, Ramana V. (2008). Reduced-order model development for airfoil forced response, International Journal of Rotating Machinery, Vol. 2008, 12 pages

[5] Ganine, Vladislav; Legrand, Mathias; Michalska, Hannah; Pierre, Christophe (2009). A sparse preconditioned iterative method for vibration analysis of geometrically mistuned bladed disks. Computers and Structures, Vol. 87, pp. 342—354.

[6] Garzon, Victor E.; Darmofal, David L. (2003) Impact of geometric variability on axial compressor performance, Journal of Turbomachinery, Vol. 125, pp. 692—703.

[7] Sinha, Alok (2008), Vibratory parameters of blades from coordinate measurement machine data. Journal of Turbomachinery. Vol. 130.

[8] Sinha, Alok (2009), Reduced-order model of a bladed rotor with geometric mistuning. Journal of Turbomachinery. Vol. 131.

[9] Sinha, Alok; Bhartiya, Yasharth (2011), Modeling geometric mistuning of a bladed rotor: Modified modal domain analysis. IUTAM Symposium on Emerging Trends in Rotor Dynamics. (Editor K. Gupta).

[10] Vishwakarma, Vinod; Sinha, Alok; Bhartiya, Yasharth; Brown, Jeffery (2013), Modified modal domain analysis of a bladed rotor using coordinate measurement machine data on geometric mistuning. Proceedings of GTE2013, ASME Turbo Expo 2013.

[11] Wagner, Nils; Helfrich, Reinhard (2015), Reliability analysis of mistuned blisks. SIRM 11th International Conference on Vibrations in Rotating Machines, Magdeburg, Germany.

[11] Wang, Shuai; Zi, Yanyang; Li, Bing; Zhang, Chunlin; He, Zhengjia (2014), Reduced-order modeling for mistuned centrifugal impellers with crack damages. Journal of Sound and Vibration, Vol. 333, pp. 6979—6995.

[12] PERMAS User's Reference manual, INTES Publication No. 450.

[13] VisPER User manual, INTES Publication No. 470.

[14] http://www.intes.de